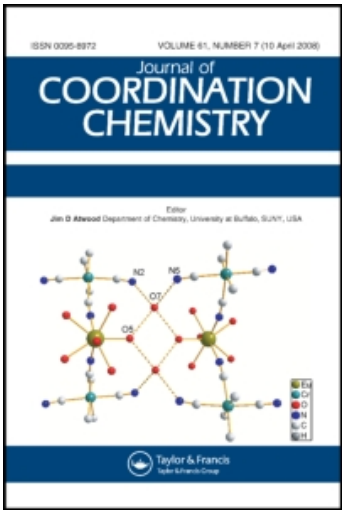

Journal of Coordination Chemistry

Publication details, including instructions for authors and subscription information:
http://www.informaworld.com/smpp/title~content=t713455674

Oxidation of pinacyanol chloride by H_2O_2 catalyzed by Fe^{III} complexed to tetraamidomacrocyclic ligand: unusual kinetics and product identification

Douglas A. Mitchell[ab]; Alexander D. Ryabov[a]; Soumen Kundu[a]; Arani Chanda[ac]; Terrence J. Collins[a]
[a] Department of Chemistry, Carnegie Mellon University, Pittsburgh, PA 15213, USA [b] Department of Chemistry and the Institute for Genomic Biology, University of Illinois at Urbana-Champaign, Urbana, IL 61801, USA [c] Eisai Inc., Andover, MA 01810, USA

First published on: 14 June 2010

To cite this Article Mitchell, Douglas A. , Ryabov, Alexander D. , Kundu, Soumen , Chanda, Arani and Collins, Terrence J.(2010) 'Oxidation of pinacyanol chloride by H_2O_2 catalyzed by Fe^{III} complexed to tetraamidomacrocyclic ligand: unusual kinetics and product identification', Journal of Coordination Chemistry, 63: 14, 2605 — 2618, First published on: 14 June 2010 (iFirst)

To link to this Article: DOI: 10.1080/00958972.2010.492426

URL: http://dx.doi.org/10.1080/00958972.2010.492426

Journal of Coordination Chemistry
Vol. 63, Nos. 14–16, 20 July–20 August 2010, 2605–2618

Oxidation of pinacyanol chloride by H_2O_2 catalyzed by Fe^{III} complexed to tetraamidomacrocyclic ligand: unusual kinetics and product identification¶

DOUGLAS A. MITCHELL†‡, ALEXANDER D. RYABOV*†, SOUMEN KUNDU†, ARANI CHANDA†§ and TERRENCE J. COLLINS*†

†Department of Chemistry, Carnegie Mellon University, 4400 Fifth Avenue, Pittsburgh, PA 15213, USA
‡Department of Chemistry and the Institute for Genomic Biology, University of Illinois at Urbana-Champaign, 1206 W. Gregory Dr, Urbana, IL 61801, USA
§Eisai Inc., 100 Federal St, Andover, MA 01810, USA

(*Received 24 January 2010; in final form 5 March 2010*)

Oxidative degradation of pinacyanol chloride (PNC) dye by H_2O_2, as catalyzed by the **1** Fe^{III}-TAML activator (TAML = tetraamidomacrocyclic ligand), occurs rapidly in water, goes to completion, and exhibits noticeably complex kinetics at pH 11. The reaction achieves a carbon mineralization of 51%. The detected products are acetate, formate, oxalate, maleate, 2-nitrobenzoate, nitrite, and nitrate. The catalytic reaction is a first-order process in **1** and the reaction rate has a Michaelis dependence in hydrogen peroxide (H_2O_2). The reaction rate increases sharply with increasing PNC concentration, reaches a maximal value, and then declines as the PNC concentration is further increased. The initial rate (v) *versus* [PNC] profile has been quantified in terms of the equation: $v = (c_1[\text{PNC}] + c_2[\text{PNC}]^2)/(c_3 + c_4[\text{PNC}] + [\text{PNC}]^2)$ which accounts for the maximum and further rate decline. Kinetic analysis at a more acidic pH (9 *vs.* 11) revealed that there is no initial rate increase and only the hyperbolic retardation by PNC is observed, in accord with the rate law $v = (b_1 + b_2[\text{PNC}])/(b_3 + [\text{PNC}])$. The kinetic data has been rationalized using the adopted mechanism of catalysis by Fe^{III}-TAML activators, which involves the reaction between **1** and H_2O_2 to form reactive, oxidized TAML (k_I, k_{-I}) followed by its reaction with the dye (k_{II}). The minimalistic addition to the scheme to account for the PNC case is the assumption that **1** may rapidly and reversibly associate with PNC (K), and the associated complex reacts also with H_2O_2 (k_{ID}, k_{-ID}) to form also the oxidized TAML. Spectral evidence for this association is presented. The optimization of PNC structure by density functional theory rules out coordination of PNC to **1** *via* the formation of a Fe–N bond. The kinetic data indicate that the rate constant k_{II} exceeds $1 \times 10^5\,(\text{mol L}^{-1})^{-1}\,\text{s}^{-1}$ at pH 11 and 25°C.

Keywords: Iron TAML complexes; Kinetics; Pinacyanol chloride; Oxidation; Hydrogen peroxide

1. Introduction

Iron(III)-tetraamidomacrocyclic ligand (TAML) activators of peroxides (**1**, scheme 1) in the solid state are square pyramidal complexes of Fe^{III} immersed into the TAML

*Corresponding authors. Email: ryabov@andrew.cmu.edu; tclu@andrew.cmu.edu
¶Dedicated to Prof: Dr Rudi van Eldik on occasion of his 65th birthday.

ISSN 0095-8972 print/ISSN 1029-0389 online © 2010 Taylor & Francis
DOI: 10.1080/00958972.2010.492426

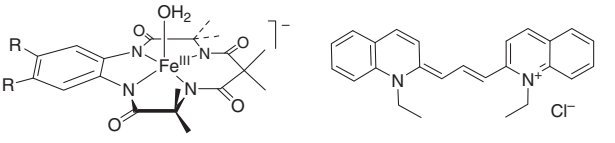

1 (**a**, R = H; **b** R = Cl) Pinacyanol chloride (PNC)

Scheme 1. Structures of the Fe^{III}-TAML activators **1** and the PNC dye used in this study.

system of four essentially planar, deprotonated amide nitrogen donors [1–3]. The axial fifth ligand is typically a halide or water. In aqueous solution, Fe^{III}-TAMLs are octahedral six-coordinate species with both axial positions occupied by water, one of which deprotonates to a hydroxo in basic solutions [4]. Fe^{III}-TAMLs are exceptional oxidation catalysts that rival the catalase–peroxidase family of enzymes in terms of catalytic performance [5]. Fe^{III}-TAMLs perform a broad variety of ''green,'' environmentally significant tasks, including the bleaching of several structurally distinct dyes [6]. Two dyes that our group has studied in significant detail are Orange II [7] and Safranin O [8]. Coincidently, the first dye that revealed the catalytic power of Fe^{III}-TAMLs through oxidation with hydrogen peroxide (H_2O_2) was pinacyanol chloride (PNC, scheme 1) [9]. The oxidative bleaching of this blue dye was fast, clean, and permitted the conclusion that Fe^{III}-TAML was a robust activator of H_2O_2 [9]. Therefore, the choice of PNC as a representative dye for kinetic characterization of the catalytic properties of Fe^{III}-TAMLs seemed logical. However, our kinetic studies of the Fe^{III}-TAML-catalyzed bleaching of PNC by H_2O_2, which were initiated almost a decade ago, resulted in unexpected, if not suspicious, observations which severely complicated the kinetic evaluation of our catalyst. We have observed that the initial rate of the Fe^{III}-TAML-catalyzed bleaching of PNC by H_2O_2 has a maximum when plotted against the PNC concentration. Such effects are more commonly found in biological systems. A well-documented example of such an effect occurs when an enzyme is inhibited by its own substrate. Substrate inhibition is routinely accounted for by a model in which the binding of a second substrate molecule to the enzyme results in the formation of a less reactive species [10, 11]. However, there exist more sophisticated explanations of the ''substrate inhibition'' phenomenon, for instance, in catalysis by peroxidase [12] and chloroperoxidase [13]. Our earlier studies have shown that these enzymes share mechanistic traits with the Fe^{III}-TAML activators [14]. Substrate inhibition is less frequently encountered in catalytic chemical systems. Rekindling our interest in substrate inhibition from artificial catalytic systems was the recent publication from van Eldik *et al.* [15] on the oxidation of Orange II by H_2O_2 in the presence of $[Fe^{III}$(octaphenylsulfonato)porphyrazine$]^{5-}$, showing that the rate of Orange II oxidation decreases with increasing concentration of the azo dye [15]. Both studies indicated that rate retardation in dye oxidation, as catalyzed by low-molecular weight compounds, could be a general phenomenon and prompted further work on the Fe^{III}-TAML-catalyzed oxidation of PNC by H_2O_2. Here, we report the results from our studies of PNC oxidation by H_2O_2 catalyzed by the Fe^{III}-TAML activator, **1a**. Our results include product identification, bleaching kinetics, and a proposed model to account for an unusually complex mechanistic regime.

PNC and related cyanine dyes are widely used in various subfields of chemistry, often being employed as photosensitizers and biomolecular probes [16, 17].

Nevertheless, there is a dearth of reports on the catalytic, oxidative degradation of pinacyanol cations [18–21]. This is surprising as these dyes also find medical application in photodynamic therapy and are also used as radiation sensitizers. Therefore, their resistance to oxidative degradation by liver cytochrome P450 enzymes [22, 23] should be considered as an important factor in drug design. Given our previous work on the similarities of Fe^{III}-TAML catalyzed reactions to that of oxidative enzymes [14], the data reported here could be viewed as a model pharmacokinetic study for the physiological degradation of PNC.

2. Experimental

The Fe^{III}-TAML complexes (**1**) were synthesized at Carnegie Mellon University as indicated previously [5, 24]. Stock solutions of **1a** were prepared (1 m mol L^{-1}, pure water). PNC was obtained from Sigma-Aldrich and used without purification. PNC stock solutions (1×10^{-4} mol L^{-1}) were prepared in 0.01 mol L^{-1} phosphate buffer at pH 9 or 11. H_2O_2 (30% v/v) was obtained from Fluka and its solutions were standardized daily by titration with ferrocene [25]. All oxidation reactions were carried out in 0.01 mol L^{-1} phosphate buffer at pH 9 and 11. Spectrophotometric and kinetic measurements were performed using a Hewlett-Packard Diode-Array spectrophotometer (model 8453) using plastic poly(methyl methacrylate) 1 cm cuvettes at 25°C. All rate measurements were done in triplicate and the initial rates reported throughout are mean values of three determinations. Initial rates of the PNC bleaching were measured at 600 nm. This wavelength corresponds to the monomeric form of the dye, which is known to form dimers and higher aggregates in water [26–28]. The aggregation results in deviations from Beer's law, and therefore an average effective extinction coefficient of 2.4×10^4 $(\text{mol L}^{-1})^{-1}$ cm^{-1} was used for calculating the initial rates. The concentration of **1a** in the reaction medium was varied in the range from 2.4×10^{-8} to 4.4×10^{-7} mol L^{-1} at pH 11 and from 9.8×10^{-8} to 9.9×10^{-7} mol L^{-1} at pH 9.

Total organic carbon (TOC) analysis was performed by Analytical Laboratory Services, Inc., Middletown, PA to determine the extent of mineralization during the bleaching of PNC by **1a**/H_2O_2. A Dionex DX500 chromatography system consisting of a GP50 gradient pump, an AS40 automated sampler, an ED40 electrochemical detector, a LC25 chromatography oven, an ASRS® 300 (P/N 064554) self-regenerating suppressor was used for ion chromatography (IC) studies. The data were analyzed using Chromeleon chromatography software (Version 6.70). The IonPac® AS9-HC (4 mm × 250 mm) analytical and IonPac® AG9-HC (4 mm × 50 mm) guard columns were obtained from Dionex. Analysis was performed under isocratic conditions with 9 m mol L^{-1} Na_2CO_3 as the mobile phase, 1 mL min^{-1} flow rate, an oven temperature of 35°C, and a SRS current of 100 mA. The injection volumes were 100 μL. The mobile phase was prepared with water from a Barnstead Nanopure system.

Density Functional Theory (DFT) calculations were carried out with the Gaussian 03 series of programs [29] within the framework of DFT [30, 31]. Our studies used the B3LYP hybrid functional [32–34] and the 6-31G basis set for all atoms. Geometry optimizations were carried out without any symmetry restrictions.

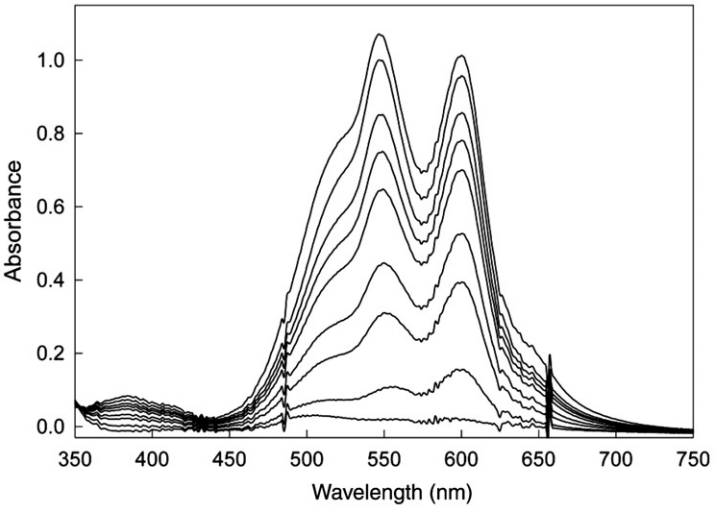

Figure 1. Spectral changes during the bleaching of PNC by H_2O_2 catalyzed by **1a** at pH 9 and 25°C. Spectra were recorded after 10, 20, 45, 60, 90, 120, 180, and 240 s, respectively. Conditions: PNC (4.9×10^{-5} mol L^{-1}), H_2O_2 (2.0×10^{-4} mol L^{-1}), and **1a** (5.0×10^{-9} mol L^{-1}) in 0.01 mol L^{-1} K-phosphate buffer.

3. Results

3.1. *Efficacy of PNC bleaching*

Spectral variations in the **1a**-catalyzed bleaching of PNC by H_2O_2 indicate complete decolorizing of the dye within 3 min (figure 1). Bleaching in the absence **1a** is negligible under identical conditions (data not shown). The catalyzed PNC bleaching is noticeably more facile than that of Orange II [7] (an azo dye) or Safranin O (a phenazine dye) [8]. The initial rate of PNC bleaching is a simple measurement, but it should be taken into consideration that the accuracy of data collected is lower than that collected for Orange II and Safranin O, because PNC has a strong tendency to aggregate and the extinction coefficient in water is dependent on dye concentration and other solution components [27, 35].

The catalytic efficacy of **1a** in terms of the *color removing stoichiometry*, that is, the number of equivalents of H_2O_2 needed for the bleaching of one equivalent of *the color* of PNC is demonstrated in figure 2. This was obtained by measuring the decrease in absorbance of PNC at 600 nm after consequent addition of aliquots of H_2O_2. The slope of a linear plot of 1.5 was obtained at three **1a** concentrations (5.4×10^{-8}, 1.6×10^{-7}, and 4.9×10^{-7} mol L^{-1}) indicating that **1a** decolorizes PNC more economically than Orange II, for which the slope of a similar plot was 0.5 [7].

3.2. *Analysis of PNC degradation fragments*

The TOC analysis of a solution from **1a**-catalyzed oxidation of PNC indicated carbon mineralization of 51%. Attempts to detect larger oxidative intermediates, both by electrospray ionization (ESI) and atmospheric pressure chemical ionization (APCI) mass-spectrometry, were not successful under a variety of experimental conditions,

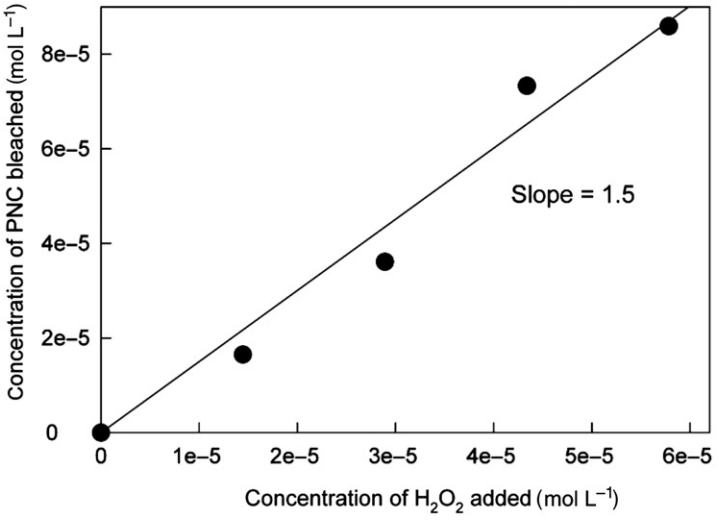

Figure 2. Stoichiometry of the PNC color removal at pH 11: amount of PNC bleached against amount of H_2O_2 added at [**1a**] 4.9×10^{-7} mol L^{-1}.

including very short reaction times ([**1a**] $(0.1 - 1.0) \times 10^{-6}$ mol L^{-1}, [H_2O_2] $(5 - 20) \times 10^{-6}$ mol L^{-1}, reaction time 1 – 10 s). Therefore, we resorted to IC to detect reaction end products (figure 3). These results provide evidence for the formation of a series of organic carboxylates (formate, acetate, oxalate, maleate, and 2-nitrobenzoate), nitrite and nitrate. These successfully identified products logically reflect the oxidatively decomposed structure of PNC (scheme 1). For example, 2-nitrobenzoate originates from the quinoline moiety of PNC. As illustrated in the chromatogram, products were identified for nearly all signals with only one significant peak remaining unidentified (marked **X**, figure 3). Subsequent analysis ruled out the possibility that fumarate, phthalates, glycolate, and 2,3-pyridinedicarboxylate comprised the unknown IC signal. Unfortunately, bigger fragments of PNC, which would be helpful in establishing a more detailed pathway of dye bleaching, were not detected by ESI or APCI. This, however, is not surprising because oxidative fragments can be more chemically fragile than the parent compound.

3.3. *Kinetics of PNC bleaching*

Our previous kinetic studies of dye bleaching by peroxides in the presence of Fe^{III}-TAML activators [5, 7, 8, 36] agree with a general mechanism of catalysis shown in scheme 2. The reactive species of the catalysts, annotated as ''oxidized TAML,'' is most likely the oxo derivative of Fe^{IV}, which has been spectrally characterized in aqueous solution [37]. Oxo-Fe^{IV}-TAML may coexist with a similar, but more reactive, Fe^{V} derivative, which has been detected in organic media [38]. All rate constants with Roman subscripts in scheme 2 are conditional, that is, they are pH-dependent. This is due to the fact that **1** in water is an octahedral diaqua species $[FeL(OH_2)_2]^-$ that will undergo deprotonation to form $[FeL(OH)(OH_2)]^{2-}$ ($pK_a = 10.1$ for **1a**) [4]. In addition, H_2O_2 ionizes with a pK_a around 11.4 [39]. Thus, these acid–base equilibria can

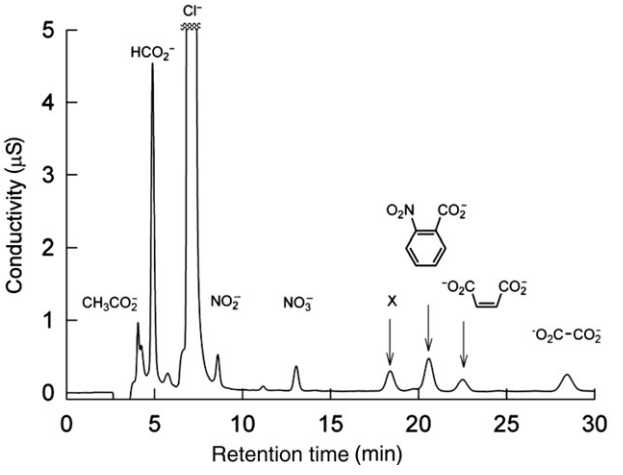

Figure 3. Ion chromatogram of products of degradation of PNC by H_2O_2 catalyzed by **1a** obtained after 10 min reaction. The reaction was quenched by the catalase enzyme (235 U mL^{-1}, pH 9). Conditions: [PNC] 0.2×10^{-3} mol L^{-1}, [H_2O_2] 2×10^{-4} mol L^{-1}, [**1a**] 2×10^{-5} mol L^{-1}, pH 9.

$$Fe^{III}\text{-TAML} + ROOH \underset{k_{-I}}{\overset{k_I}{\rightleftharpoons}} \text{(Oxidized TAML)}$$

$$\text{(Oxidized TAML)} + \text{Dye} \xrightarrow{k_{II}} Fe^{III}\text{-TAML} + \text{Primary Product}$$

$$\text{Primary Product} \xrightarrow{fast} \rightarrow \rightarrow \text{Final Product(s)}$$

Scheme 2. A general mechanism of catalysis by Fe^{III}-TAMLs.

dramatically affect the values of k_I. Derivation of a rate law from the elementary reactions shown in scheme 2 leads to equation (1), where the rate constant k_{-I} is negligible because the condition $k_{-I} \ll k_I[\text{ROOH}] + k_{II}[\text{Dye}]$ holds under all possible scenarios. First-order kinetics in **1a** hold at pH 9 and 11, that is, under the conditions when the dominating species are the diaqua $[FeL(OH_2)_2]^-$ and the aqua/hydroxo $[FeL(OH)(OH_2)]^{2-}$ complexes, respectively. We have also confirmed that first-order dependence in **1a** holds at different concentrations of PNC, for example, 6.1×10^{-6} and 4.9×10^{-5} mol L^{-1} at pH 9.

$$-\frac{d[\text{Dye}]}{dt} = \frac{k_I k_{II}[\text{ROOH}][\text{Dye}][Fe^{IIITAML}]}{k_{-I} + k_I[\text{ROOH}] + k_{II}[\text{Dye}]}. \quad (1)$$

Equation (1) predicts hyperbolic growth in the rate of PNC decolorizing as the concentration of H_2O_2 is increased. This effect has been confirmed and the data are presented in figure 4. As illustrated, the initial rate levels off at higher H_2O_2 concentrations and the dependences are consistent with the empirical rate law shown in equation (2). Fitting the experimental data to equation (2) allowed calculation of effective parameters a_1 and a_2 of equation (2), which are summarized in table 1. The solid lines in figure 4 are the calculated dependences using the best-fit values of a_1 and a_2.

$$-\frac{d[\text{PNC}]}{dt} = \frac{a_1[\text{ROOH}]}{a_2 + [\text{ROOH}]}. \quad (2)$$

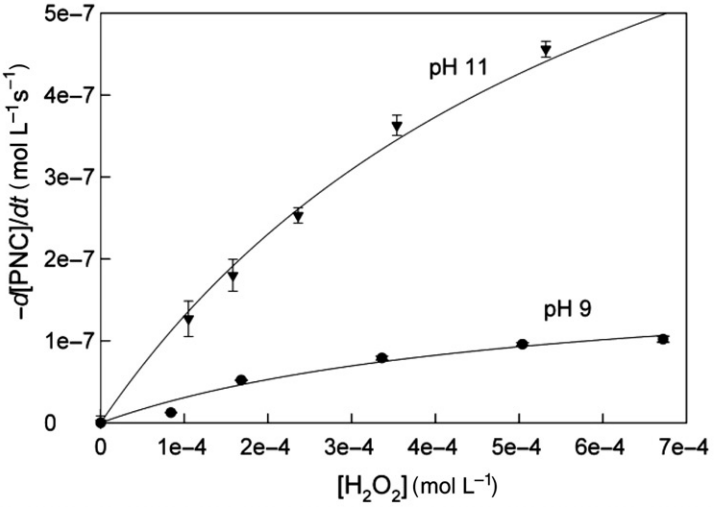

Figure 4. Dependence of the initial rate of PNC bleaching on H_2O_2 concentration at pH 9 and 11 (0.01 M phosphate); [**1a**] 9.9×10^{-8} mol L^{-1}, [PNC] 9.8×10^{-5} mol L^{-1}, 25°C.

Table 1. Effective kinetic parameters calculated in this work by fitting experimental data to equations (2)–(4); 25°C, 0.01 mol L^{-1} phosphate.

Effective parameter	pH 9	pH 11	Concentrations of reagents (mol L^{-1})	Meaning of parameters in terms of equation (6)
a_1 (mol L^{-1}) s^{-1}	$(1.9 \pm 0.5) \times 10^{-7}$	$(9.8 \pm 0.8) \times 10^{-7}$	**1a**: 9.9×10^{-8}	k_{II}[PNC][**1**]
a_2 (mol L^{-1})	$(5 \pm 2) \times 10^{-4}$	$(6.5 \pm 0.9) \times 10^{-4}$	PNC: 9.8×10^{-5}	$\frac{(k_{-ID}+k_{II})[PNC](\mathbf{1}+K[PNC])}{k_I+k_{ID}K[PNC]}$
b_1 (mol L^{-1})^2 s^{-1}	$(1.2 \pm 0.2) \times 10^{-2}$		**1a**: 4.9×10^{-8}	$\frac{k_I k_{II}[ROOH][\mathbf{1}]}{(k_{-ID}+k_{II})K}$
b_2 (mol L^{-1}) s^{-1}	$(3.3 \pm 0.2) \times 10^{-8}$		H_2O_2: 1.68×10^{-4}	$\frac{k_{ID}k_{II}[ROOH][\mathbf{1}]}{k_{-ID}+k_{II}}$
b_3 (mol L^{-1})	$(5.9 \pm 1.8) \times 10^{-6}$			$\frac{\mathbf{1}}{K}+\frac{k_{ID}[ROOH]}{(k_{-ID}+k_{II})}$
c_1 (mol L^{-1})^2 s^{-1}		$(3.8 \pm 1.7) \times 10^{-12}$	**1a**: 1.0×10^{-8}	$\frac{k_I k_{II}[ROOH][\mathbf{1}]}{(k_{-ID}+k_{II})K}$
c_2 (mol L^{-1}) s^{-1}		$\sim 1.4 \times 10^{-16}$	H_2O_2: 1.7×10^{-4}	$\frac{k_{ID}k_{II}[ROOH][\mathbf{1}]}{k_{-ID}+k_{II}}$
c_3 (mol L^{-1})^2		$(3.5 \pm 1.0) \times 10^{-10}$		$\frac{k_I[ROOH]}{(k_{-ID}+k_{II})K}$
c_4 (mol L^{-1})		~ 0		$\frac{\mathbf{1}}{K}+\frac{k_{ID}[ROOH]}{(k_{-ID}+k_{II})}$

Measurements of the rates of PNC bleaching at variable dye concentrations indicated that the general equation (1) does not hold for PNC. Although equation (1) predicts the rate growth, the data in figure 5 obtained at pH 9 show that the initial rate *decreases* hyperbolically as the PNC concentration increases, in accordance with equation (3). The solid line in figure 5 is the calculated curve using the best-fit effective values of b_1, b_2, and b_3, which are summarized in table 1.

$$-\frac{\mathrm{d[PNC]}}{\mathrm{d}t} = \frac{b_1 + b_2[\mathrm{PNC}]}{b_3 + [\mathrm{PNC}]}. \tag{3}$$

A parallel experiment, carried out at pH 11, exhibited even more complex PNC dependence. As seen in figure 6, the reaction rate first increases sharply at low PNC

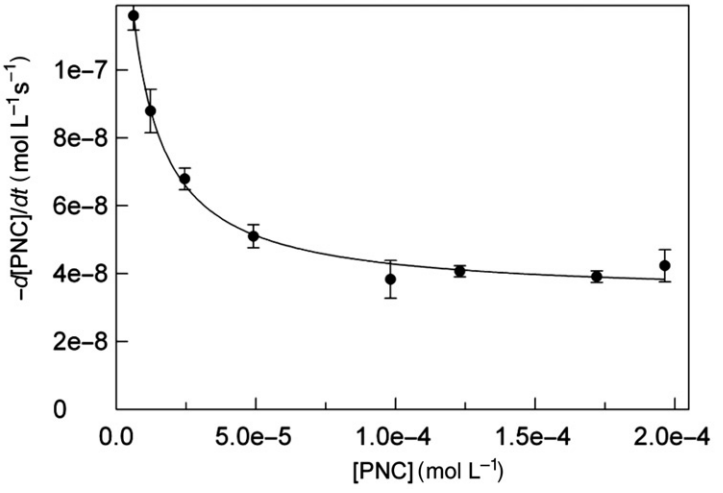

Figure 5. Initial rate of the **1a**-catalyzed PNC bleaching by H_2O_2 as a function of the dye concentration at pH 9. Conditions: [**1a**] 4.9×10^{-8} mol L^{-1}, [H_2O_2] 1.7×10^{-4} mol L^{-1}, 25°C, 0.01 mol L^{-1} phosphate.

concentrations, reaches a maximal value, and then decreases gradually as the dye concentration continues to grow. At low [PNC], when the rate rises with increasing [PNC], the kinetic data agree with general equation (1). For the rest of the plot, there is an obvious disagreement for higher concentrations of PNC. These data demonstrate that more than one kinetic pathway is operating during the **1a**-catalyzed oxidation of PNC, which depends on the PNC concentration. Kinetic profiles with maxima, such as the one shown in figure 6, are accountable in terms of equations similar to

$$-\frac{\mathrm{d[PNC]}}{\mathrm{d}t} = \frac{c_1[\mathrm{PNC}] + c_2[\mathrm{PNC}]^2}{c_3 + c_4[\mathrm{PNC}] + [\mathrm{PNC}]^2}. \quad (4)$$

The experimental data in figure 6 were fitted to equation (4), and the solid line in figure 6 is the simulated curve using the best-fit effective values $c_1 - c_4$ which are included in table 1.

3.4. *Spectral evidence for association between Fe^{III}-TAML and PNC*

The complex formation between Fe^{III}-TAML and PNC was confirmed at pH 7.3 by **1b**, the pK_a value of which equals 10.0 [4]. The spectral evidence was obtained using aqua, $[FeL(OH_2)_2]^-$, not hydroxo species, because OH^-, as compared to H_2O, is a much poorer leaving ligand [40]. The results obtained using a tandem quartz cell[†2] are demonstrated in figure 7. As seen, the intensity of strong PNC bands at 550 and 600 nm are moderately increased by solution of **1b** (taken in excess relative to PNC) after its addition to the second cell compartment without mixing with a PNC solution. Immediately after mixing, the intensity of the PNC bands rapidly decreased by 50% and continued to decline for another 5 min, after which the spectrum did not change further.

This reaction did not involve H_2O_2, therefore spectral changes are not attributable to oxidative degradation of PNC. By the time a complex between **1b** and PNC had achieved

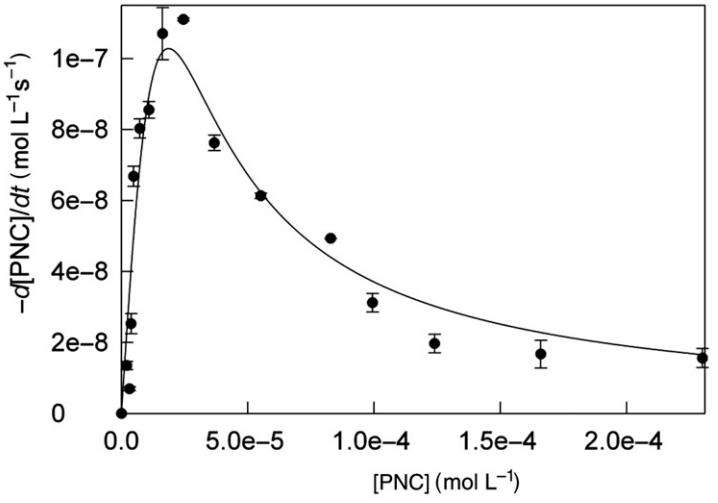

Figure 6. Initial rate of the **1a**-catalyzed PNC bleaching by H_2O_2 as a function of the dye concentration at pH 11. Conditions: [**1a**] 10^{-8} mol L^{-1}, [H_2O_2] 1.7×10^{-4} mol L^{-1}, 25°C, 0.01 mol L^{-1} phosphate.

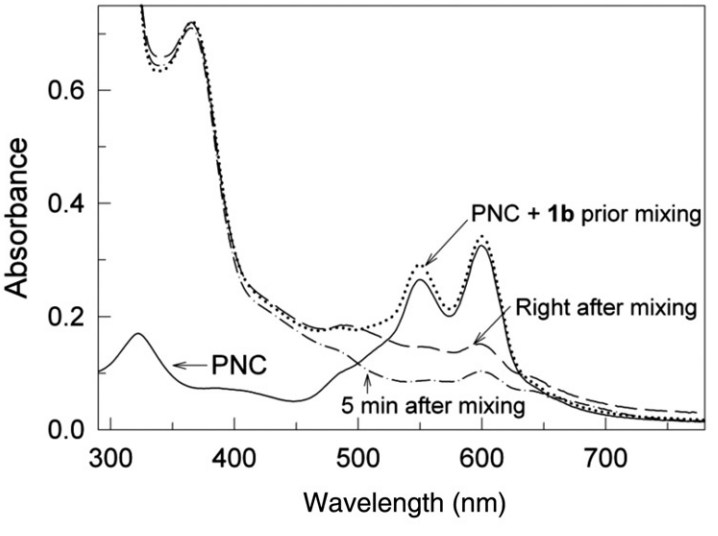

Figure 7. Illustration of the association between the Fe^{III}-TAML activator **1b** and PNC in aqueous solution using a tandem UV-Vis cell separated by a quartz wall. The solid line is the spectrum of *ca* 3×10^{-5} mol L^{-1} solution of PNC added to the first compartment of the tandem cell. The dotted line is the spectrum recorded after adding 3×10^{-4} mol L^{-1} solution of **1b** to the second compartment without mixing PNC and **1b**. The dashed line was obtained right after mixing PNC and **1b**. The dash-dotted spectrum is the final spectrum that was recorded 5 min after mixing. Conditions: 25°C, pH 7.3. See text for more details.

equilibrium, a new shoulder had developed at *ca* 660 nm and a profound, three-fold decrease in absorbance at 600 nm, was clearly evident.

$$Fe^{III}\text{-TAML} + PNC \underset{}{\overset{K}{\rightleftharpoons}} \{Fe^{III}\text{-TAML,PNC}\}$$

$$Fe^{III}\text{-TAML} + ROOH \underset{k_{-I}}{\overset{k_I}{\rightleftharpoons}} (\text{Oxidized TAML})$$

$$\{Fe^{III}\text{-TAML,PNC}\} + ROOH \underset{k_{-ID}}{\overset{k_{ID}}{\rightleftharpoons}} (\text{Oxidized TAML}) + PNC$$

$$(\text{Oxidized TAML}) + \text{Dye} \xrightarrow{k_{II}} Fe^{III}\text{-TAML} + \text{Primary Product}$$

$$\text{Primary Product} \xrightarrow{fast} \rightarrow \rightarrow \text{Final Product(s)}$$

Scheme 3. A minimalistic mechanism of Fe^{III}-TAML-catalyzed oxidation of the pinacyanol dye by H_2O_2 that accounts for the substrate inhibition.

4. Discussion

4.1. *Stoichiometric mechanism of the catalyzed oxidation of PNC*

Pinacyanol cations form adducts with many chemicals and therefore, it should not be surprising that the PNC cation binds to **1**, which will carry a charge −1 or −2, depending on the solution pH. It is reasonable to assume that this fast, non-covalent interaction influences the kinetics of PNC bleaching. Therefore, scheme 2 required a correction for "the PNC case" to rationalize the results highlighted in figures 5 and 6. In particular, two steps, the pre-equilibrium binding of PNC to **1** and the interaction of the ensuing {Fe^{III}-TAML, PNC} adduct with H_2O_2 to form the reactive species (oxidized TAML) and free PNC, are included in scheme 3. This scheme represents a minimalistic version of the mechanism sufficient to account for our experimental observations. For mathematical simplicity, our model assumed that PNC did not associate with oxidized TAML.

The expression for the rate of PNC bleaching in the presence of **1** and peroxides (equation (5)) was derived from scheme 3. The steady-state approximation with respect to the oxidized TAML was applied and the mass balance equation for all iron-containing species ([**1**] = [Fe^{III}-TAML] + [Fe^{III}-TAML, PNC] + [oxidized TAML]) was used.

$$-\frac{d[PNC]}{dt} = \frac{\left(k_1[PNC] + k_{ID}K[PNC]^2\right)k_{II}[ROOH][\mathbf{1}]}{k_{-I} + k_1[ROOH] + k_{ID}K[ROOH][PNC] + (k_{-ID} + k_{II})[PNC] + (k_{-ID} + k_{II})K[PNC]^2}. \quad (5)$$

The rate constant k_{-I}, which appears in the denominator, has previously been found to be negligible [5, 7, 36]. Therefore, equation (5) simplifies to equation (6), which is qualitatively consistent with the experimental data in figures 4–6 and the corresponding equations (2)–(4).

$$-\frac{d[PNC]}{dt} = \frac{\left(k_1[PNC] + k_{ID}K[PNC]^2\right)k_{II}[ROOH][\mathbf{1}]}{k_1[ROOH] + k_{ID}K[ROOH][PNC] + (k_{-ID} + k_{II})[PNC] + (k_{-ID} + k_{II})K[PNC]^2}. \quad (6)$$

In particular, equation (6) predicts the Michaelis-type dependence on the concentration of H_2O_2. This is consistent with equation (2). The meaning of the calculated parameters a_1 and a_2 in terms of equation (6) is described in table 1; a_1 permits estimation of the rate constant, k_{II}, for the interaction between the oxidized form of **1a** and PNC, which equals 2.0×10^4 and $1.0 \times 10^5 (\text{mol L}^{-1})^{-1} \text{s}^{-1}$ at pH 9 and 11, respectively.

Equation 6 agrees with equation (3) on the assumption that the first term in the equation (6) denominator, k_I[ROOH], is negligible compared with the sum of all other terms. Thus, equation (6) can be simplified and rewritten as equation (3). The meaning of parameters $b_1 - b_3$ is shown in table 1. Supporting this is the observation that the value of k_I at pH 9 is noticeably lower than that at pH 11 [5]. This dependence is reminiscent of a result described by the van Eldik *et al.* [15] for oxidation of Orange II by H_2O_2 in the presence of [Fe^{III}(octaphenylsulfonato)porphyrazine]$^{5-}$.

Rationalization of the extremal rate dependence on PNC concentration (figure 6 and equation (4)) requires the complete version of equation (6). The experimentally measured parameters, $c_1 - c_4$ (table 1), indicate that k_{II} can be calculated from the ratio c_1/c_3 as approximately $10 \times 10^5 (\text{mol L}^{-1})^{-1} \text{s}^{-1}$. Although it is somewhat larger than the value obtained through the use of equation (2), we assume that the match is acceptable when taking into consideration the following: (i) the minimalistic nature of scheme 3 for interpreting the data in figure 6, (ii) uncertainty in determining four parameters $c_1 - c_4$ of equation (4), (iii) the tendency of PNC to self associate in water, and (iv) deviations from Beer's law for this dye.

4.2. *On the nature of {Fe^{III}-TAML, PNC} adduct*

The four deprotonated amide nitrogen donors surrounding iron(III) in **1** are strong "electron pumps" that render axial ligation of Fe^{III} very difficult in aqueous solution. For example, the equilibrium constants for binding of chloride K_{Cl} and pyridine K_{py} to the diaqua form of **1a** equal 0.18 [4] and $4.7 (\text{mol L}^{-1})^{-1}$ [41], respectively. PNC is a nitrogen-containing dye that would be expected to interact with **1a** in a manner similar to pyridine. Thus, the value of $K_{py} = 4.7 (\text{mol L}^{-1})^{-1}$ could be considered as an approximation for PNC binding capacity to **1a** *via* nitrogen donor. Our data presented in figures 5 and 6 rule out nitrogen ligation because the concentration ranges of PNC used were around $10^{-4} \text{mol L}^{-1}$, which is considerably lower than 0.2mol L^{-1} (the inverse of the equilibrium constant K_{py}). Thus, PNC most likely adopts a binding mode independent of nitrogen. Computational data support this conjecture. Optimization of the PNC structure by DFT (figure 8) also indicates that the coordination of the nitrogen donor to iron(III) of **1** is problematic. The nitrogens of PNC are nearly equivalent and the rings are to a great extent, aromatic. Both nitrogens have considerable sp^2 character and both N–CH_2Me bonds are virtually in the plane of the quinoline rings. This, as mentioned above, will sterically preclude Fe–N bond formation. Therefore, we propose that the interaction between **1** and PNC is of a different nature.

Pinacyanol cations bind to numerous targets in water, including DNA [17], metal cations [42–44], and tungstate [45]. The stoichiometry of PNC binding to the tungsten species at pH 3–4 is unusual, with a molar ratio of PNC : W equal to 1 : 2 and 1 : 3 [45]. These examples indicate that the pinacyanol dye may bind to metal-containing and other molecules *via* different mechanisms, the nature of which is dictated by a particular target.

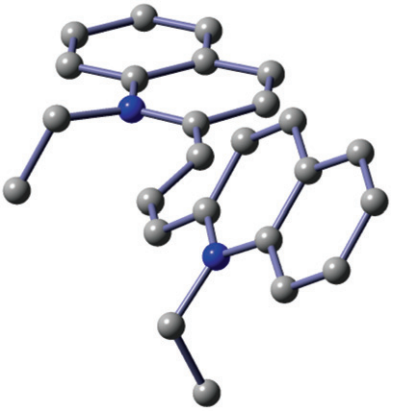

Figure 8. DFT optimized structure of PNC (nitrogens are shown in blue and hydrogens are omitted for clarity).

Regarding the Fe^{III}-TAMLs, we favor pi-stacking (as in DNA). The electrostatic mechanism (as in tungstate) in water seems least probable. Unfortunately, none of these weak interactions can be reliably probed by DFT and previous attempts to co-crystallize the complex have been unsuccessful. Therefore, the precise nature of the interaction between **1** and PNC cannot be reliably established at this time.

4.3. *Final remarks*

This work, in conjunction with a recent report from the van Eldik *et al.* [15], indicates that low-molecular weight activators of peroxide may suffer from noticeable substrate inhibition when the substrate is a polyaromatic, cationic dye. Our previous studies on **1a**-catalyzed bleaching of Orange II, a polyaromatic, *anionic* dye, found no indication of substrate inhibition [7, 8]. The charge of the [Fe^{III}(octaphenylsulfonato) porphyrazine]$^{5-}$ catalyst [15] is significantly more negative than that of **1**, but still, Orange II binds stronger to the former due to the repulsion between the anionic dye and the pi-system of Fe^{III}-TAML. The binding constant of $2.2 \times 10^3\,(\mathrm{mol\,L^{-1}})^{-1}$ reported (pH 10) is rather high compared to that for bromide ($1.2\,\mathrm{M^{-1}}$) [15]. Most likely, the binding is relatively non-specific, pi-cation interaction for **1** and PNC. Therefore, dyes may affect the catalytic activity of small oxidation catalysts and compromise their performance. This possibility should be taken into consideration when designing catalytic formulations.

Acknowledgments

Support is acknowledged from the Heinz Endowments (Terrence J. Collins), the C.E. Kaufman Foundation (T.J.C.), the Alexander von Humboldt foundation (Alexander D. Ryabov), and the National Institutes of Environmental Health Sciences (B.B., 5R01-ES015849). We thank Riddhi Roy for her assistance in

calculations and Hauck Environmental Engineering Laboratories, Carnegie Mellon University for providing access to the IC instrument.

References

[1] T.J. Collins. *Acc. Chem. Res.*, **27**, 279 (1994).
[2] T.J. Collins. *Acc. Chem. Res.*, **35**, 782 (2002).
[3] T.J. Collins, C. Walter. *Sci. Am.*, **294**, 83–88, 90 (2006).
[4] A. Ghosh, A.D. Ryabov, S.M. Mayer, D.C. Horner, D.E. Prasuhn Jr, S. Sen Gupta, L. Vuocolo, C. Culver, M.P. Hendrich, C.E.F. Rickard, R.E. Norman, C.P. Horwitz, T.J. Collins. *J. Am. Chem. Soc.*, **125**, 12378 (2003).
[5] A. Ghosh, D.A. Mitchell, A. Chanda, A.D. Ryabov, D.L. Popescu, E. Upham, G.J. Collins, T.J. Collins. *J. Am. Chem. Soc.*, **130**, 15116 (2008).
[6] T.J. Collins, S.K. Khetan, A.D. Ryabov. In *Chemistry and Applications of Iron-TAML Catalysts in Green Oxidation Processes Based on Hydrogen Peroxide*, P.T. Anastas, R.H. Crabtree (Eds), pp. 39–77, Wiley-VCH Verlag GmbH & KgaA, Weinheim (2009).
[7] N. Chahbane, D.-L. Popescu, D.A. Mitchell, A. Chanda, D. Lenoir, A.D. Ryabov, K.-W. Schramm, T.J. Collins. *Green Chem.*, **9**, 49 (2007).
[8] A. Chanda, A.D. Ryabov, S. Mondal, L. Alexandrova, A. Ghosh, Y. Hangun-Balkir, C.P. Horwitz, T.J. Collins. *Chem. Eur. J.*, **12**, 9336 (2006).
[9] C.P. Horwitz, D.R. Fooksman, L.D. Vuocolo, S.W. Gordon-Wylie, N.J. Cox, T.J. Collins. *J. Am. Chem. Soc.*, **120**, 4867 (1998).
[10] A. Cornish-Bowden. *Fundamentals of Enzyme Kinetics*, Portland Press, London (1995).
[11] A. Fersht. *Structure and Mechanism in Protein Science: A Guide to Enzyme Catalysis and Protein Folding*, Freeman, NY (1999).
[12] M. Dequaire, B. Limoges, J. Moiroux, J.-M. Saveant. *J. Am. Chem. Soc.*, **124**, 240 (2002).
[13] A.N. Shevelkova, Y.I. Sal'nikov, N.L. Kuźmina, A.D. Ryabov. *FEBS Lett.*, **383**, 259 (1996).
[14] A.D. Ryabov, T.J. Collins. *Adv. Inorg. Chem.*, **61**, 471 (2009).
[15] A. Theodoridis, J. Maigut, R. Puchta, E.V. Kudrik, R. van Eldik. *Inorg. Chem.*, **47**, 2994 (2008).
[16] A. Mishra, R.K. Behera, P.K. Behera, B.K. Mishra, G.B. Behera. *Chem. Rev.*, **100**, 1973 (2000).
[17] B.A. Armitage. *Top. Curr. Chem.*, **253**, 55 (2005).
[18] R.G. Bhirud, E.V. Srisankar, K.S. Narayan. *Proc. Indian Acad. Sci., Chem. Sci.*, **103**, 83 (1991).
[19] M.H. Robbins, R.S. Drago. *J. Catal.*, **170**, 295 (1997).
[20] S.R. Segal, S.L. Suib, L. Foland. *Chem. Mater.*, **9**, 2526 (1997).
[21] T. Yamada, S. Shinoda, K. Kikawa, A. Ichimura, J. Teraoka, T. Takui, H. Tsukube. *Inorg. Chem.*, **39**, 3049 (2000).
[22] P.H. Roos, N. Jakubowski. *Anal. Bioanal. Chem.*, **392**, 1015 (2008).
[23] U.M. Zanger, M. Turpeinen, K. Klein, M. Schwab. *Anal. Bioanal. Chem.*, **392**, 1093 (2008).
[24] Available online at: www.chem.cmu.edu/groups/collins/awardpatpub/patents/index.html.
[25] V.N. Goral, M.I. Nelen, A.D. Ryabov. *Anal. Lett.*, **28**, 2139 (1995).
[26] L.D. Derkacheva. *Izv. Akad. Nauk SSSR, Ser. Fiz.*, **20**, 410 (1956).
[27] W. West, S. Perace. *J. Phys. Chem.*, **69**, 1894 (1965).
[28] R. Sabate, J. Estelrich. *Spectrochim. Acta A Mol. Biomol. Spectrosc.*, **70**, 471 (2008).
[29] M.J. Frisch, G.W. Trucks, H.B. Schlegel, G.E. Scuseria, M.A. Robb, J.R. Cheeseman, J. Montgomery, J.A.T. Vreven, K.N. Kudin, J.C. Burant, J.M. Millam, S.S. Iyengar, J. Tomasi, V. Barone, B. Mennucci, M. Cossi, G. Scalmani, N. Rega, G.A. Petersson, H. Nakatsuji, M. Hada, M. Ehara, K. Toyota, R. Fukuda, J. Hasegawa, M. Ishida, T. Nakajima, Y. Honda, O. Kitao, H. Nakai, M. Klene, X. Li, J.E. Knox, H.P. Hratchian, J.B. Cross, V. Bakken, C. Adamo, J. Jaramillo, R. Gomperts, R.E. Stratmann, O. Yazyev, A.J. Austin, R. Cammi, C. Pomelli, J.W. Ochterski, P.Y. Ayala, K. Morokuma, G.A. Voth, P. Salvador, J.J. Dannenberg, V.G. Zakrzewski, S. Dapprich, A.D. Daniels, M.C. Strain, O. Farkas, D.K. Malick, A.D. Rabuck, K. Raghavachari, J.B. Foresman, J.V. Ortiz, Q. Cui, A.G. Baboul, S. Clifford, J. Cioslowski, B.B. Stefanov, G. Liu, A. Liashenko, P. Piskorz, I. Komaromi, R.L. Martin, D.J. Fox, T. Keith, M.A. Al-Laham, C.Y. Peng, A. Nanayakkara, M. Challacombe, P.M.W. Gill, B. Johnson, W. Chen, M.W. Wong, C. Gonzalez, J.A. Pople, *Gaussian 03 (release B.05)*, Gaussian, Inc., Wallingford CT (2004).
[30] R.G. Parr, W. Yang. *Density-functional Theory of Atoms and Molecules*, Clarendon, NY (1989).
[31] T. Ziegler. *Chem. Rev.*, **91**, 651 (1991).
[32] A.D. Becke. *J. Chem. Phys.*, **98**, 5648 (1993).
[33] C. Lee, W. Yang, R.G. Parr. *Phys. Rev. B: Condens. Matter*, **37**, 785 (1988).

[34] P.J. Stephens, F.J. Devlin, C.F. Chabalowski, M.J. Frisch. *J. Phys. Chem.*, **98**, 11623 (1994).
[35] S. Barazzouk, H. Lee, S. Hotchandani, P.V. Kamat. *J. Phys. Chem. B*, **104**, 3616 (2000).
[36] D.-L. Popescu, A. Chanda, M.J. Stadler, S. Mondal, J. Tehranchi, A.D. Ryabov, T.J. Collins. *J. Am. Chem. Soc.*, **130**, 12260 (2008).
[37] A. Chanda, X. Shan, M. Chakrabarti, W. Ellis, D. Popescu, F. Tiago de Oliveria, D. Wang, L. Que Jr, T.J. Collins, E. Münck, E.L. Bominaar. *Inorg. Chem.*, **47**, 3669 (2008).
[38] F. Tiago de Oliveira, A. Chanda, D. Banerjee, X. Shan, S. Mondal, L. Que Jr, E.L. Bominaar, E. Münck, T.J. Collins. *Science*, **315**, 835 (2007).
[39] C.W. Jones. *Applications of Hydrogen Peroxide and Derivatives*, The Royal Society of Chemistry, Cambridge (1999).
[40] R. van Eldik. *Inorganic High Pressure Chemistry. Kinetics and Mechanisms*, Vol. 7, Elsevier, NY (1986).
[41] V. Polshin, D.-L. Popescu, A. Fischer, A. Chanda, D.C. Horner, E.S. Beach, J. Henry, Y.-L. Qian, C.P. Horwitz, G. Lente, I. Fabian, E. Münck, E.L. Bominaar, A.D. Ryabov, T.J. Collins. *J. Am. Chem. Soc.*, **130**, 4497 (2008).
[42] K.I. Pokrovskaya, I.I. Levkoev, S.V. Natanson. *Zh. Fiz. Khim.*, **30**, 161 (1956).
[43] E.V. Vasil'eva. *Zh. Anal. Khim.*, **2**, 167 (1947).
[44] A.K. Babko, E.V. Vasiléva. *Zh. Anal. Khim.*, **2**, 159 (1947).
[45] P.P. Turov, D.S. Turova. *Zh. Anal. Khim.*, **25**, 934 (1970).